

# Violation of a Bell-like inequality in single-neutron interferometry

Yuji Hasegawa<sup>1</sup>, Rudolf Loidl<sup>1,2</sup>, Gerald Badurek<sup>1</sup>, Matthias Baron<sup>1,2</sup> & Helmut Rauch<sup>1</sup>

<sup>1</sup>Atominstytut der Österreichischen Universitäten, Stadionallee 2, A-1020 Wien, Austria

<sup>2</sup>Institute Laue Langevin, B. P. 156, F-38042 Grenoble Cedex 9, France

**Non-local correlations between spatially separated systems have been extensively discussed in the context of the Einstein, Podolsky and Rosen (EPR) paradox<sup>1</sup> and Bell's inequalities<sup>2</sup>. Many proposals and experiments designed to test hidden variable theories and the violation of Bell's inequalities have been reported<sup>3-7</sup>; usually, these involve correlated photons, although recently an experiment was performed with <sup>9</sup>Be<sup>+</sup> ions<sup>8</sup>. Nevertheless, it is of considerable interest to show that such correlations (arising from quantum mechanical entanglement) are not simply a peculiarity of photons. Here we measure correlations between two degrees of freedom (comprising spatial and spin components) of single neutrons; this removes the need for a source of entangled neutron pairs, which would present a considerable technical challenge. A Bell-like inequality is introduced to clarify the correlations that can arise between observables of otherwise independent degrees of freedom. We demonstrate the violation of this Bell-like inequality: our measured value is  $2.051 \pm 0.019$ , clearly above the value of 2 predicted by classical hidden variable theories<sup>9-12</sup>.**

The concept of quantum non-contextuality<sup>9-12</sup> represents a straightforward extension of the classical view: the result of a particular measurement is determined independently of previous (or simultaneous) measurements on any set of mutually commuting observables<sup>13</sup>. Local theories represent a particular circumstance of non-contextuality, in that the result is assumed not to depend on measurements made simultaneously on spatially separated (mutually non-interacting) systems. In order to test non-contextuality, joint measurements of commuting observables that are not necessarily separated in space are required.

Two degrees of freedom can be used for such experiments, for example, the spatial and the spinor properties, of single particles, prepared in a non-factorized state and manipulated to measure two commuting observables. A Bell-like inequality has been obtained to distinguish non-contextual hidden variable (NCHV) theories from the prediction of quantum mechanics<sup>14</sup>.

Here, we report a single-neutron interferometer experiment to show stronger correlations than the classical non-contextual model with the use of a Bell-like inequality. (General descriptions of neutron interferometer experiments are summarized in the literature<sup>15</sup>.) We note that all the experiments showing the violation of the Bell's inequalities have been performed with correlated entangled pairs<sup>16-20</sup>, including the recent one with <sup>9</sup>Be<sup>+</sup> ions<sup>8</sup>. We used not entangled pairs but single neutrons and the entanglement is achieved between different degrees of freedom in a single particle. This is based on the fact that states of spin-1/2 particles, like neutrons, are described by a tensor product Hilbert space, that is,  $H = H_1 \otimes H_2$  where  $H_1$  and  $H_2$  are respectively disconnected Hilbert spaces corresponding to the spatial and the spinor wave function. Observables of the spatial part are commutable with those of the spinor part, this justifying the derivation of a Bell-like inequality by the NCHV theories<sup>14</sup>. The experiment consists of joint measurements of commuting observables of single neutrons in an appropriately prepared nonfactorizable state.

In our polarized neutron interferometer experiment, the total wavefunction consists of the entanglement of the spatial part and

the spinor part<sup>21</sup>, that is, different degrees of freedom. The normalized total wavefunction  $|\Psi\rangle$  can be represented as a Bell state,  $|\Psi\rangle = \frac{1}{\sqrt{2}}(|\downarrow\rangle \otimes |I\rangle + |\uparrow\rangle \otimes |II\rangle)$ . Here,  $|\uparrow\rangle$  and  $|\downarrow\rangle$  denote the up-spin and down-spin states, and  $|I\rangle$  and  $|II\rangle$  denote the two beam paths in the interferometer.

The expectation value for the joint measurement for the spinor  $\frac{1}{\sqrt{2}}(|\uparrow\rangle + e^{i\alpha}|\downarrow\rangle)$  and the path  $\frac{1}{\sqrt{2}}(|I\rangle + e^{i\chi}|II\rangle)$  is calculated to be:

$$E'(\alpha, \chi) = \langle \Psi | \hat{P}^s(\alpha) \cdot \hat{P}^p(\chi) | \Psi \rangle \\ = \langle \Psi | [(+1) \cdot \hat{P}_{\alpha,+1}^s + (-1) \cdot \hat{P}_{\alpha,-1}^s] \\ [(+1) \cdot \hat{P}_{\chi,+1}^p + (-1) \cdot \hat{P}_{\chi,-1}^p] | \Psi \rangle \quad (1)$$

where  $\hat{P}_{\alpha\pm 1}^s$  and  $\hat{P}_{\chi\pm 1}^p$  are the projection operators to the states  $\frac{1}{\sqrt{2}}(|\uparrow\rangle \pm e^{i\alpha}|\downarrow\rangle)$  and  $\frac{1}{\sqrt{2}}(|I\rangle \pm e^{i\chi}|II\rangle)$ , respectively. (These projection operators and the expectation value correspond to  $P_{\pm}(\mathbf{a})$ ,  $P_{\pm}(\mathbf{b})$  and  $E(\mathbf{a}, \mathbf{b})$  in the conventional EPR argument<sup>22</sup>.) It should be emphasized here that the observables  $\hat{P}^s$  and  $\hat{P}^p$  operate in different Hilbert spaces, and thus commute each other.

A Bell-like inequality for a single-neutron experiment is expressed<sup>14</sup> with the expectation values  $E'(\alpha, \chi)$  as  $-2 \leq S' \leq 2$ , with  $S' \equiv E'(\alpha_1, \chi_1) + E'(\alpha_1, \chi_2) - E'(\alpha_2, \chi_1) + E'(\alpha_2, \chi_2)$ .

In our experiments, the expectation value  $E'(\alpha, \chi)$  has been determined by a combination of count rates in a single detector with appropriate setting of  $\chi$  and  $\alpha$ . This is given by:

$$E'(\alpha, \chi) \\ = \frac{N'(\alpha, \chi) + N'(\alpha + \pi, \chi + \pi) - N'(\alpha, \chi + \pi) - N'(\alpha + \pi, \chi)}{N'(\alpha, \chi) + N'(\alpha + \pi, \chi + \pi) + N'(\alpha, \chi + \pi) + N'(\alpha + \pi, \chi)} \quad (2)$$

where  $N'(\alpha_j, \chi_k)$  denotes the count rate with the spin-rotation of  $\alpha_j$  and the phase shift of  $\chi_k$ , which is given by  $N'(\alpha_j, \chi_k) = \langle \Psi | \hat{P}_{\alpha_j,+1}^s \cdot \hat{P}_{\chi_k,+1}^p | \Psi \rangle$ . This accounts for measurements to determine the expectation value of the joint measurement with successive counts in one detector.

Quantum theory predicts sinusoidal behaviour for the count rate  $N'^{\text{qm}}(\alpha, \chi) = \frac{1}{2}\{1 + \cos(\alpha + \chi)\}$ . The same behaviour is also expected for the expectation value  $E'(\alpha, \chi) = \cos(\alpha + \chi)$ . These functions will show the violation of the Bell-like inequality for various sets of the polarization analysis ( $\alpha$ ) and the phase shift ( $\chi$ ). The maximum violation is expected, for instance, for the set,  $\alpha_1 = 0$ ,  $\alpha_2 = \pi/2$ ,  $\chi_1 = \pi/4$ , and  $\chi_2 = -\pi/4$ , as  $S' = 2\sqrt{2} = 2.82 > 2$ . So far we have described the experiment in terms of perfect implementation. In the actual experiment, however, perfect sinusoidal dependence of  $N'$  cannot be established owing to unavoidable component misalignments, imperfect quality of polarization/interference, and so on, which is characterized by contrasts of the oscillations. The value,  $S'$ , reduces in proportion to these contrasts. Thus, average contrasts of more than 70.7% ( $= \sqrt{2}/2$ ) is essential in order to show the violation of the Bell-like inequality.

Our experiments consist of three stages: preparation, manipulation and detection. The preparation was achieved by the use of a spin-turner after the polarized beam was split into two, producing a Bell state,  $|\Psi_{\text{exp}}\rangle = \frac{1}{\sqrt{2}}(|\rightarrow\rangle \otimes |I\rangle + |\leftarrow\rangle \otimes |II\rangle)$ . In the manipulation, two parameters of  $\chi$  and  $\alpha$  were adjusted. And finally, neutrons with certain properties were detected. In recent work, four detectors were used to measure the total outcomes of Stern-Gerlach polarization analysers installed in both interfering beams<sup>14</sup>. But it is shown that polarization analysis of the O-beam is sufficient to obtain correlation coefficients.

The experiment was carried out at the silicon-perfect-crystal interferometer beam line S18 at the high flux reactor at the Institute Laue Langevin<sup>23</sup>. A schematic view of the experimental set-up is shown in Fig. 1. The neutron beam was monochromatized to have a

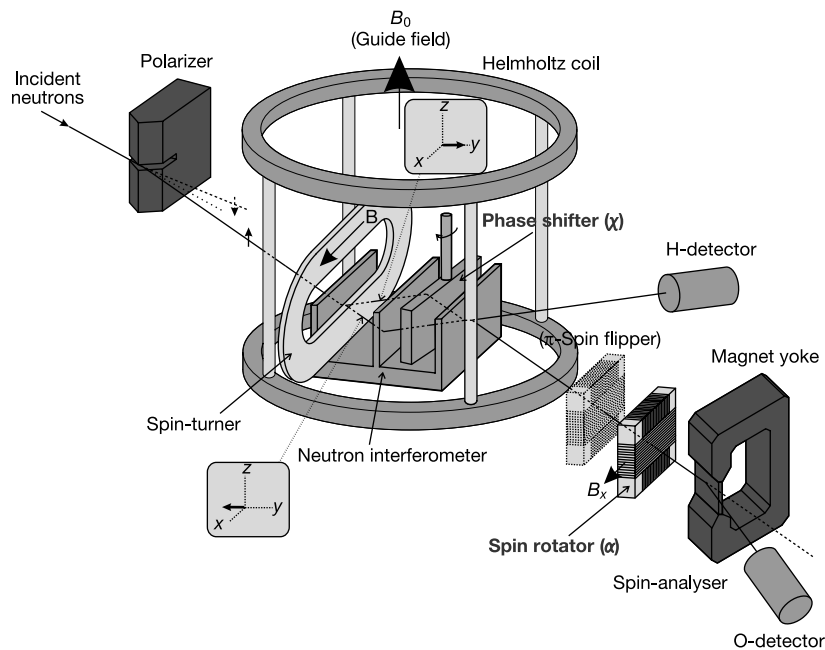


**Figure 1** Schematic view of the experimental set-up to observe quantum correlations clarified by the Bell-like inequality in single-neutron interferometry. The experiments consists of three processes. (1) Preparation of the entangled state  $|\Psi_{\text{exp}}\rangle = \frac{1}{\sqrt{2}}(|\rightarrow\rangle\otimes|I\rangle + |\leftarrow\rangle\otimes|II\rangle)$ : an incident neutron beam is polarized with the use of a magnetic-prism polarizer. This up-polarized beam falls on the silicon-perfect-crystal neutron interferometer and splits into two beam paths,  $|I\rangle$  and  $|II\rangle$ . A  $\mu$ -metal

spin-turner directs  $|\uparrow\rangle$  to  $|\rightarrow\rangle$  for one beam and to  $|\leftarrow\rangle$  for the other. (2) Manipulation of the two parameters: a phase shift  $\chi$  and a spinor rotation angle  $\alpha$  are adjusted. Together with a Heusler spin-analyser, neutrons with particular spinor and path properties are selected, resulting in  $\hat{\rho}_{\alpha,+1}^s \cdot \hat{\rho}_{\chi,+1}^p |\Psi\rangle$ . (3) Detection: numbers of neutrons are counted, yielding  $N'(\alpha, \chi) = \langle \Psi | \hat{\rho}_{\alpha,+1}^s \cdot \hat{\rho}_{\chi,+1}^p | \Psi \rangle$ .

mean wave length of  $\lambda_0 = 1.92(2) \text{ \AA}$  by the use of a silicon perfect crystal monochromator. This incident beam was polarized vertically by magnetic-prism refractions, then entering a triple-Laue interferometer. This interferometer was adjusted to 220 reflections. A parallel-sided plate was used as a phase shifter (varying  $\chi$ ). A pair of water-cooled Helmholtz coils produced a fairly uniform magnetic guide field,  $B_0 + \hat{z}$ , around the interferometer. A magnetically saturated Heusler crystal together with a rectangular spin rotator (adjusting  $\alpha$ ) and a spin flipper, if necessary, enabled the selection of neutrons with certain polarization directions.

A crucial optical element in our preparation is a spin turner, which turns the incident spinor  $|\uparrow\rangle$  to  $|\rightarrow\rangle$  in one beam and to  $|\leftarrow\rangle$  in the other. For this procedure, we used a soft-magnetic  $\mu$ -metal sheet<sup>24</sup>, which gives high permeability induced by weak magnetic fields. We used a sheet of 0.5 mm thick in an oval ring form and two DC-coils to magnetize this soft-magnetic sheet.

In the manipulation, the important parameters are the relative phase,  $\chi$ , between the two beams and the spinor rotation angle,  $\alpha$ . To show the capability of our manipulation, we measured interference oscillations for two two-level systems in the interferometer: one for a spatial (path), and the other for spinor (spin). Typical oscillations are shown in Fig. 2. Sinusoidal oscillations occur when varying the parameters  $\chi$ , in Fig. 2a, and  $\alpha$ , in Fig. 2b. Sufficiently high contrasts were achieved to confirm the fact that we established an apparatus for manipulating two subsystems: the path and the spin of neutrons in the interferometer.

A maximum violation of the Bell-like inequality is expected in setting the spinor rotation angle  $\alpha$  at  $0, \pi/2, \pi$  and  $3\pi/2$ . Typical intensity modulations, obtained by varying the phase shift  $\chi$ , are shown in Fig. 3. Contrasts evidently decreased from those shown in Fig. 2, mainly because of dephasing/depolarization at the  $\mu$ -metal spin-turner. A gradual reduction of contrast by increasing  $\alpha$  is attributed to slight depolarization by the spinor-rotator and the

$\pi$ -spin-flipper. We, however, managed to obtain enough high contrasts, more than 70.7%, to accomplish the experiment. The  $\mu$ -metal spin-turner induces additional relative phase shift between two beams in the interferometer, so all interference oscillations are shifted by about  $\pi$  in this figure. We took this shift into account in determining appropriate  $\chi$ -positions to show the maximum violation.

After fitting to sinusoidal dependence by the least-squares method, the expectation values  $E_{\text{obs}}$  were calculated using equation (2). The typical statistical error of  $E_{\text{obs}}$  was  $\pm 0.01$ , obtained from curves of a single measurement. We repeated the same measurements at least 16 times to reduce statistical errors. The final value of  $E_{\text{obs}}$  and its error were evaluated by the weighted average of all measurements. So, the final errors are the sum of systematic and statistical errors. (The main reason for systematic error was phase instability, random drift of phase, during the measurement.) We obtained  $E_{\text{obs}}(0, 0.79\pi)$  to be  $0.542 \pm 0.007$  from the intensities of  $N'(0, 0.79\pi)$ ,  $N'(\pi, 0.79\pi)$ ,  $N'(0, 1.79\pi)$ , and  $N'(\pi, 1.79\pi)$ . In the same manner, we determined  $E_{\text{obs}}(0, 1.29\pi) = 0.4882 \pm 0.012$ ,  $E_{\text{obs}}(0.5\pi, 0.79\pi) = -0.538 \pm 0.006$ , and  $E_{\text{obs}}(0.5\pi, 1.29\pi) = 0.438 \pm 0.012$ . In evaluating the Bell-like inequality,  $S'$  was calculated to be  $2.051 \pm 0.019 > 2$ , for  $\alpha_{1,2} = 0, 0.50\pi$ , and  $\chi_{1,2} = 0.79\pi, 1.29\pi$ . This clearly shows a violation of the Bell-like inequality: stronger correlations than the classical non-contextual model.

The results above were obtained using a neutron detector of more than 99% efficiency. In this case, however, a fair-sampling hypothesis is still required, because of losses in the interferometer—the second plate of the interferometer is not a mirror but a beam-splitter—in addition to the fact that the count rates were obtained successively one after another. (It should be mentioned that equation (2) itself does not use this assumption.) A similar experiment concerning the non-contextual hidden variable theories

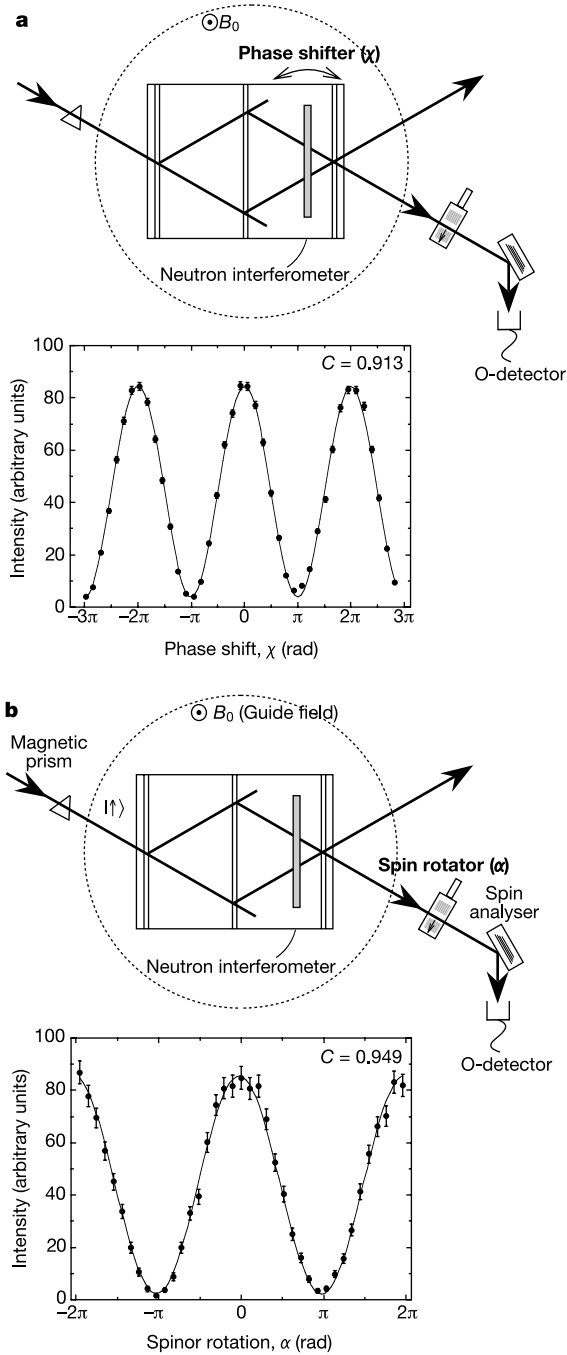


**Figure 2** Interference oscillations for two-level systems. **a**, Spatial Hilbert-spaces; **b**, polarization Hilbert-spaces. Contrasts of over 91% for **a** and about 95% for **b** were achieved. This confirmed the quality of our manipulation for the path and spinor properties.

with entangled photons<sup>25</sup> was reported. In this experiment, a ‘trigger’ instead of a polarized incident beam was used to show correlations in coincidence counting. This leaves the total system in an entangled state, potentially one of four states with equal probabilities. Thus, the ‘projection’ postulate in the mixed state is needed to deduce the quantum contextuality from this experiment.

The correlations observed in our experiments could be discussed in terms of a semiclassical wave theory, that is, as beam polarizations, as frequently used in optics. This calculation exhibits a non-factorizable total polarization by  $P^S(\alpha)$  for the spin manipulations

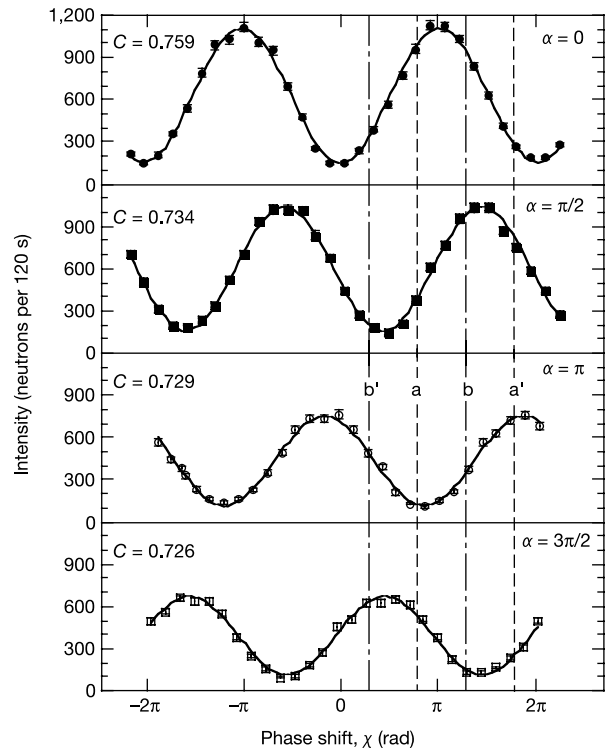


**Figure 3** Typical interference oscillations with spinor rotation angle  $\alpha = 0, \pi/2, \pi$  and  $3\pi/2$ . Contrasts of 76% for one and about 73% for the other three were achieved. Expectation values,  $E_{\text{obs}}$ , were derived from the intensities of appropriate  $\chi$ : on line  $a$   $\chi = 0.79\pi$ , on line  $a'$   $\chi = 1.79\pi$ , on line  $b$   $\chi = 1.29\pi$ , and on line  $b'$   $\chi = 0.29\pi$ , where a maximum violation of the Bell-like inequality is expected. These values exhibited the final  $S'$  value of  $2.051 \pm 0.019 > 2$ , which indicates a clear violation of the Bell-like inequality.

and  $P^P(\chi)$  for the path manipulations. We note here that the entanglement is not limited to different particles but is generally applicable to different degrees of freedom in single particles. General arguments on the entanglement-induced correlation can be found in the literature<sup>26,27</sup>. □

Received 1 April; accepted 25 June 2003; doi:10.1038/nature01881.

- Einstein, A., Podolsky, B. & Rosen, N. Can quantum-mechanical description of physical reality be considered complete? *Phys. Rev.* **47**, 777–780 (1935).
- Bell, J. S. On the Einstein-Podolsky-Rosen paradox. *Physics* **1**, 195–200 (1964).
- Clauser, J. F., Horne, M. A., Shimony, A. & Holt, R. A. Proposed experiment to test local hidden-variable theories. *Phys. Rev. Lett.* **23**, 880–884 (1969).
- Clauser, J. F. & Shimony, A. Bell's theorem: experiment tests and implications. *Rep. Prog. Phys.* **41**, 1881–1927 (1978).
- Mann, A. & Revzen, M. (eds) *The Dilemma of Einstein* Vol. 12, *Podolsky and Rosen: 60 Years Later* (Annals of the Israel Physical Society, The Institute of Physics, Bristol, 1996).
- Afriat, A. & Selleri, F. (eds) *The Einstein, Podolsky and Rosen Paradox in Atomic, Nuclear and Particle Physics* (Plenum, New York, 1999).
- Bertlmann, R. A. & Zeilinger, A. (eds) *Quantum [Un]speakeables* (Springer, Berlin/Heidelberg/New York, 2002).
- Rowe, M. A. *et al.* Experimental violation of a Bell's inequality with sufficient detection. *Nature* **409**, 791–794 (2001).
- Bell, J. S. On the problem of hidden variables in quantum mechanics. *Rev. Mod. Phys.* **38**, 447–452 (1966).
- Kochen, S. & Specker, E. P. The problem of hidden variables in quantum mechanics. *J. Math. Mech.* **17**, 59–87 (1967).
- Mermin, N. D. Simple unified form for the major no-hidden-variables theorems. *Phys. Rev. Lett.* **65**, 3373–3376 (1990).
- Mermin, N. D. Hidden variables and the two theorems of John Bell. *Rev. Mod. Phys.* **65**, 803–815 (1993).
- Roy, S. M. & Singh, V. Quantum violation of stochastic noncontextual hidden-variable theories. *Phys. Rev. A* **48**, 3379–3381 (1993).
- Basu, S., Bandyopadhyay, S., Kar, G. & Home, D. Bell's inequality for single spin-1/2 particle and quantum contextuality. *Phys. Lett A* **279**, 281–286 (2001).
- Rauch, H. & Werner, S. A. *Neutron Interferometry* (Clarendon, Oxford, 2000).
- Freedman, S. J. & Clauser, J. F. Experimental test of local hidden-variable theories. *Phys. Rev. Lett.* **28**,

938–941 (1972).  
 17. Aspect, A., Grangier, P. & Roger, G. Experimental realization of Einstein-Podolsky-Rosen-Bohm gedanken experiment: A new violation of Bell's inequalities. *Phys. Rev. Lett.* **49**, 91–94 (1982).  
 18. Ou, Z. Y. & Mandel, L. Violation of Bell's inequality and classical probability in a two-photon correlation experiment. *Phys. Rev. Lett.* **61**, 50–53 (1988).  
 19. Tittel, W., Brendel, J., Zbinden, H. & Gisin, N. Violation of Bell inequalities by photons more than 10 km apart. *Phys. Rev. Lett.* **81**, 3563–3566 (1998).  
 20. Weihs, G., Jennewein, T., Simon, C., Weinfurter, H. & Zeilinger, A. Violation of Bell's inequality under strict Einstein locality conditions. *Phys. Rev. Lett.* **81**, 5039–5043 (1998).  
 21. Sakurai, J. *Modern Quantum Mechanics* 203 (Addison-Wesley, Reading, Massachusetts, 1994).  
 22. Aspect, A. in *The Wave-Particle Dualism* (eds Diner, S., Farque, D., Lochak, G. & Selleri, F.) 377 (D. Reidel Publishing Company, Dordrecht, 1984).  
 23. Kroupa, G. *et al.* Basic features of the upgraded S18 neutron interferometer set-up at ILL. *Nucl. Instrum. Meth. A* **440**, 604–608 (2000).  
 24. Rauch, H., Wilfing, A., Bauspiess, W. & Bonse, U. Precise determination of the 4 pi-periodicity factor of a spinor wave function. *Z. Phys. B* **29**, 281–284 (1978).  
 25. Michler, M., Weinfurter, H. & Zukowski, M. Experiments towards falsification of noncontextual hidden variable theories. *Phys. Rev. Lett.* **84**, 5457–5461 (2000).  
 26. Englert, B.-G. Remark on some basic issues in quantum mechanics. *Z. Naturforsch.* **54a**, 11–32 (1999).  
 27. Bell, J. S. in *Themes in Contemporary Physics II* (eds Deser, S. & Finkelstein, R. J.) 1 (World Scientific, Singapore, 1989).

**Acknowledgements** We appreciate discussions with R. A. Bertlmann, I. J. Cirac and D. Home. This work has been supported by the Austrian Fonds zur Förderung der Wissenschaftlichen Forschung.

**Competing interests statement** The authors declare that they have no competing financial interests.

**Correspondence** and requests for materials should be addressed to Y.H. (hasegawa@ati.ac.at).

## Entangled quantum state of magnetic dipoles

S. Ghosh<sup>1</sup>, T. F. Rosenbaum<sup>1</sup>, G. Aeppli<sup>2</sup> & S. N. Coppersmith<sup>3</sup>

<sup>1</sup>James Franck Institute and Department of Physics, University of Chicago, Chicago, Illinois 60637, USA

<sup>2</sup>London Centre for Nanotechnology and Department of Physics and Astronomy, University College London, London WC1E 6BT, UK, and NEC Laboratories, 4 Independence Way, Princeton, New Jersey 08540, USA

<sup>3</sup>Department of Physics, University of Wisconsin, Madison, Wisconsin 53706, USA

Free magnetic moments usually manifest themselves in Curie laws, where weak external magnetic fields produce magnetizations that vary as the reciprocal of the temperature ( $1/T$ ). For a variety of materials that do not display static magnetism, including doped semiconductors<sup>1</sup> and certain rare-earth intermetallics<sup>2</sup>, the  $1/T$  law is replaced by a power law  $T^{-\alpha}$  with  $\alpha < 1$ . Here we show that a much simpler material system—namely, the insulating magnetic salt  $\text{LiHo}_x\text{Y}_{1-x}\text{F}_4$ —can also display such a power law. Moreover, by comparing the results of numerical simulations of this system with susceptibility and specific-heat data<sup>3</sup>, we show that both energy-level splitting and quantum entanglement are crucial to describing its behaviour. The second of these quantum mechanical effects—entanglement, where the wavefunction of a system with several degrees of freedom cannot be written as a product of wavefunctions for each degree of freedom—becomes visible for remarkably small tunnelling terms, and is activated well before tunnelling has visible effects on the spectrum. This finding is significant because it shows that entanglement, rather than energy-level redistribution, can underlie the magnetic behaviour of a simple insulating quantum spin system.

The insulator that we focus on in the search for the cause of the anomalous power-law divergence of the magnetic susceptibility is  $\text{LiHo}_x\text{Y}_{1-x}\text{F}_4$ , a salt where magnetic  $\text{Ho}^{3+}$  ions are randomly

substituted for nonmagnetic  $\text{Y}^{3+}$  with probability  $x$ . For  $x = 1$ , the material is the dipolar-coupled ferromagnet,  $\text{LiHoF}_4$ , with a Curie temperature of 1.53 K. Randomly distributing dipoles in a solid matrix provides quenched disorder, while the angular anisotropy of the dipole–dipole interaction leads to competition between ferromagnetic and antiferromagnetic bonds and the possibility of many (nearly) degenerate ground states<sup>4</sup>. Indeed, the low-temperature magnetic phase diagram of the dipolar-coupled rare-earth tetrafluorides progresses smoothly from long-range order to glassiness with increasing spin dilution<sup>3</sup>. What interests us here, however, is the considerably diluted  $x = 0.045$  compound, where we have observed<sup>5,6</sup>—contrary to classical expectations<sup>4</sup>—novel ‘antiglass’ behaviour as well as long-lived spin oscillations whose qualitative understanding seems to require mesoscopic quantum coherence. We show in Fig. 1 the experimental d.c. susceptibility,  $\chi$ , plotted against temperature,  $T$ , for a single-crystal specimen of the material. What emerges is not the standard Curie law,  $1/T$ , expected for non-interacting magnetic moments, but instead a diverging response following a power law  $T^{-\alpha}$ , with  $\alpha = 0.75 \pm 0.01$ . This power law is close to that associated with the diverging local susceptibilities inferred for doped silicon<sup>1</sup> as well as metallic rare-earth materials<sup>2</sup> on the brink of magnetic order. What is most striking, however, is that the magnetic susceptibility for  $\text{LiHo}_{0.045}\text{Y}_{0.955}\text{F}_4$  is a smoothly diverging quantity, even though the magnetic specific heat ( $C$ , Fig. 2a) is characterized by unusually sharp peaks in the same temperature range. In ordinary materials containing magnetic ions, there is a strong correlation between magnetic susceptibility and specific heat in the sense that anomalies, especially as strong as the

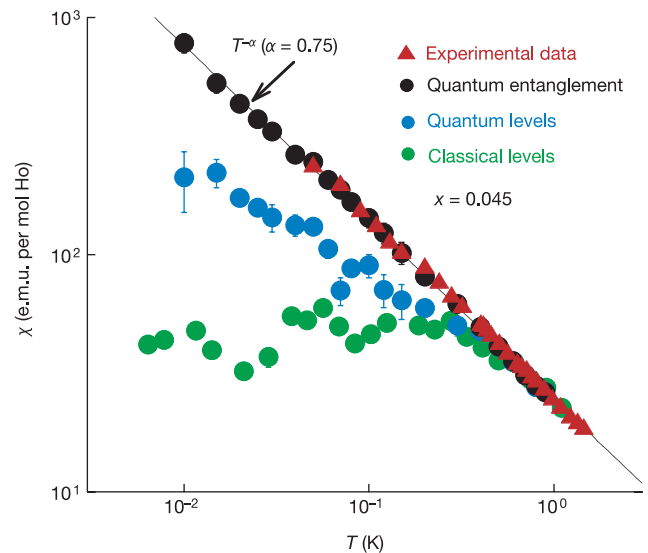


**Figure 1** Magnetic susceptibility  $\chi$  versus temperature  $T$  of the diluted, dipolar-coupled Ising magnet,  $\text{LiHo}_{0.045}\text{Y}_{0.955}\text{F}_4$ . Red triangles, experimental data; filled circles, simulations. Green circles, classical decimation when the calculations are performed with  $g_{\perp} = 0$ . Blue circles, susceptibility computed using the classical procedure, equation (3), of determining Curie constants by adding (subtracting) moments when the ground state is predominantly ferromagnetic (antiferromagnetic), but with quantum decimation, using energy levels derived from the full dipolar Hamiltonian of equation (1). Although the susceptibility approaches that of the experiment more closely than before, it still deviates by at least a factor of four at low temperatures. Black circles, use of quantum decimation as well as the correct quantum mechanical form of susceptibility given by equation (5), using the entanglement of the low-lying energy doublet with the excited states. The line is a best fit to  $\chi(T) \propto T^{-\alpha}$ , with  $\alpha = 0.75 \pm 0.01$ . Although  $\alpha$  is always less than 1, it is not a universal number. It varies from 0.62 to 0.81 as the concentration  $x$  decreases from 0.1 to 0.01, a trend also observed in Heisenberg systems<sup>7</sup>. The simulation results have not been scaled, and agree quantitatively with the experimental results.